Asian Journal of Chemistry Vol. 22, No. 4 (2010), 2953-2958

Hydrothermal Preparation and Characterization of Nanocrystalline TiO_2 Powder and its Photocatalytic Degradation of Alizarin Salt Dye Under UV-Light

OGUZHAN AVCIATA*, FIGEN SAHIN, IBRAHIM ERDEN and ULVI AVCIATA
Department of Chemistry, Faculty of Arts and Sciences,
Yildiz Technical University, Esenler-34210, Istanbul, Turkey
E-mail: ierden@yildiz.edu.tr

Titanium dioxide (TiO_2) can be used as a photocatalyst because of its semiconductor property. In this work, pure anatase-TiO_2 nanoparticles were synthesized by hydrothermally process at 210 ºC in 90 min. The structural and physico-chemical properties of anatase-nano-titanium dioxide were determined by powder XRD, FTIR, BET and SEM analyses. Titanium dioxide particles were coated to the stainless steel plates by dip coating technique. The photocatalytic performance of the mono layer coated plates were tested for degradation of alizarin salt dye in solution under UV-light.

Key Words: Nano TiO_2, Hydrothermal process, Photocatalysis, Dye.

INTRODUCTION

Nanocrystalline TiO_2, one of the most popular photocatalyst because of its high photosensivity, non-toxicity, easy availability, strong oxidation power and long-term stability[1,2]. Titanium dioxide powder must be used with ultraviolet light ($\lambda <$ 387 nm) to destroy the organic pollutants. TiO_2 is widely used to photodegradate many organic pollutants for its relatively high catalytic reactivity, strong oxidation power, long-term stability against photocorrosion and chemical corrosion[3-5]. Titanium dioxide has three kinds of phase structures. These are anatase, rutile and brookite. Anatase as a metastable phase usually exhibits the most photocatalytic active due to low recombination rate of photo-generated electrons and holes[6-8]. On the contrary, the most stable rutile phase is least active or not active at all. So anatase has higher photocatalytic activity than others[9]. BET specific surface areas, good crystallization and relative small crystallite size are important to improve the photocatalytic activity[3].

The term hydrothermal came from the earth sciences, where it implied a regime of high temperatures and water pressures. Hydrothermal synthesis controls the thermodynamic and no thermodynamic variables[10,11]. In recent years, hydrothermal synthesis is used in the synthesis of various inorganic materials to control grain size, particle morphology, microstructures, phase composition and surface chemical properties[12,13]. Moreover, the hydrothermal process is environmentally friendly since the reactions are carried out in a closed system and the contents can be recovered and reused after the synthesis[14].

Textile dyes and other industrial dyestuffs constitute one of the largest groups of organic compounds. If they do not discharge in environment without any treatment, they can cause skin problems and harmful for humans. In many cases, the efficiency of photocatalytic degradation has been demonstrated on various kinds of dyes *i.e.* azo, reactive, cationic dyes. That textile dyes can be degraded in the presence of TiO_2 powder as a photocatalyst under strong ultraviolet light[15-19].

In this study, nanocrystalline TiO_2 particles were synthesized by the hydrothermal process. The coating solution was prepared and TiO_2 particles were coated to the stainless steel plates. The plates were used in the photocatalytic system. Their photocatalytic characteristic is measured by UV-vis spectrophotometer. Alizarin salt dye was used as a dye which is frequently encountered in wastewater as a dangerous organic pollutant[20-24].

EXPERIMENTAL

As starting precursors, the following reagents were employed: tetrapropylorthotitanate [$Ti(OPr^I)_4$, was as a TiO_2 source; hydrochloride acid (Merck, 37.0 %) as catalyst; 2-butoxyethanol (Merck, 99.9 %) and propane-2-ol (Merck, 99.0 %) as solvent. Deionized water as hydrolysis agent; 3-glycidoxypropyltrimethoxysilane (GLYMO) and tetraethlyorthosilicate.

Berghoff model hydrothermal unit interfaced with a temperature controller and timer unit was used for synthesizing of nano-TiO_2 photocatalyst. The crystalline phase of the nano-TiO_2 particles was analyzed by X-ray powder diffraction (XRD) obtained from Rigaku Geigerflex D Max/B model X-ray diffractometer. The crystalline size of the nano-TiO_2 was calculated from the X-ray diffraction peak according to the Scherer's equation: $dhkl = k\lambda/[\beta\cos(2\theta)]$, where dhkl is the average crystalline size (nm), λ is the wavelength of the CuKα radiation applied ($\lambda = 0.154$ nm), θ is the Bragg's angle of diffraction, β is the full-width at half maximum intensity of the peak observed at $2\theta = 25.3°$ and k is a constant usually applied as *ca.* 0.94.

Surface morphologies of the particles were investigated using scanning electron microscopy (SEM, Jeol Model), BET surface area, average pore diameter were determined by using quantachrome BET analyzer. Malyern analyzer was used for measure the particle size in the solid phase. Dye concentration in the aqueous solution after irradiation was measured by a Agilent 8453 model UV-vis-NIR spectrophotometer.

Synthesis of nanocrystalline TiO_2: Tetrapropylorthotitanate, $Ti(OPr^I)_4$ was used as starting material and dissolved in propane-2-ol and stirred for 10 min at ambient temperature. A hydrochloride acid solution was added into alkoxide solution by burette at the rate of 1 mL/min and continued to stir for 10 min. The reaction solution was stirred until a homogeneous solution formed at ambient temperature. Then, the deionized water was added into the reaction solution by burette at the rate of 1 mL/min The molar ratio of $H_2O/Ti(OPr^I)_4$ and $HCl/Ti(OPr^I)_4$ were 1.5 and 0.3. Sol-solution was then transferred to the stainless steel teflon autoclave. After this,

autoclave was removed from the hydrothermal unit and cooled to room temperature. Hydrothermal reactions were conducted at 210 ºC for 90 min. Powders were centrifuged and dried in a vacuum sterilizer at 60 ºC for 5 h to obtain the nano-TiO_2 powder.

Coating of nano-TiO_2 powder: 3-Glycidoxypropyltrimethoxysilane (GLYMO) was first reacted with TEOS for 10 min (GLYMO/TEOS: 1) then EtOH was added to this mixture. After stirring 10 min, the mixture was solved and HCl and deionized water were added into the mixture. After stirring 10 min, dispersed nano-TiO_2 (1 g) was added to the solution and stirred for 10 min. Finally, 2-butoxyethanol was added into the last solution and that solution was stirred for 24 h to obtain good dispersed coating solution. Finally transparent and colorless solution was obtained. The ethanol, HCl, deionized water, 2-butoxyethanol to tetraethylorthosilicate mol/mol ratios were 10.5; 0.05; 6.3 and 0.05, respectively. Stainless steel plate surfaces were coated with this solution using dip-coating apparatus at 12 inch/min speed. The nano-TiO_2 coated plates were cured in the vacuum oven at 80 ºC for 1 h.

Photocatalytic degradation of alizarine salt dye: The photocatalytic performance of the films was determined by the degradation of alizarine dye solution. The coated stainless steel plate was immersed into alizarin dye solution with a concentration of 0.5 mg/L at pH:6. The alizarine dye solution was circulated into the stainless steel plates at the ambient temperature. Two 15 W UV lamp with a primary wavelength at 365 nm was used in the photocatalytic system. The change of alizarin salt dye concentration was measured by UV-vis spectrophotometer.

RESULTS AND DISCUSSION

Characterization of the nano-TiO_2: The crystalline phase of hydrothermally synthesized TiO_2 sample was analyzed by XRD. Fig. 1 shows XRD patterns of the TiO_2 powders prepared by hydrothermal method at 210 ºC for 90 min. The XRD pattern of the nano-TiO_2 was compared with PDF-021-1272 data files and all the sharp peaks observed in the XRD pattern belong to anatase phase of TiO_2. The other crystalline forms of TiO_2, rutile and brookite, have not been detected.

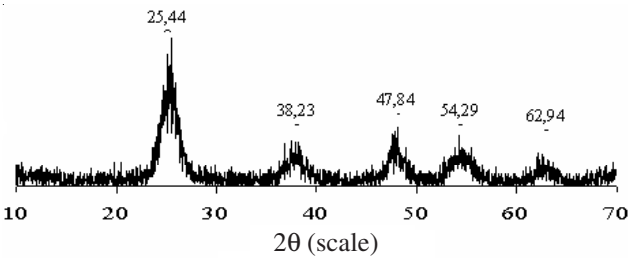

Fig. 1. XRD pattern of hydrothermally synthesized TiO_2 crystalline

The average crystalline size of the nano-TiO_2 was measured 10 nm by applying Scherer equation. BET surface area is 65.0 m^2/g and bigger than other available Titania's.

SOME PHYSICAL CHARACTERISTICS OF SYNTHESIZED TiO_2 CRYSTALLINE

Crystal size	10.126 nm
Grain size	65.0 m^2/g

SEM and EDS analysis's were showed the synthesized structure is anatase phased TiO_2 (Figs. 2a-b and 3). Aggregation is occurred when the powder TiO_2 is become damp from air. The main causes of agglomeration are small and mild particles and the variable electrical charges in the atmosphere. The aggregation may result from pH control, calibrated zeta potential values and usage of high frequency ultrasonic mixer. A typical SEM micrograph of the nano-TiO_2, as-synthesized, shown in Fig. 2, indicates that the particles are spherical in nature. It seems that hydrothermal synthesis causes spherical particles of the nano-TiO_2 crystallites virtually at equivalent sizes. Particle size distribution is observed nanometer scales in the aqua atmosphere (Fig. 4). The particles are fully anatase formed and easily dispersed in water.

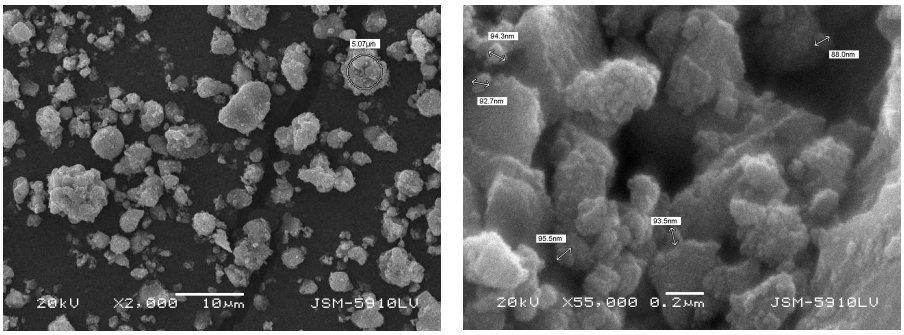

Fig. 2a-b. SEM microphotograph of the nano-TiO_2 particle

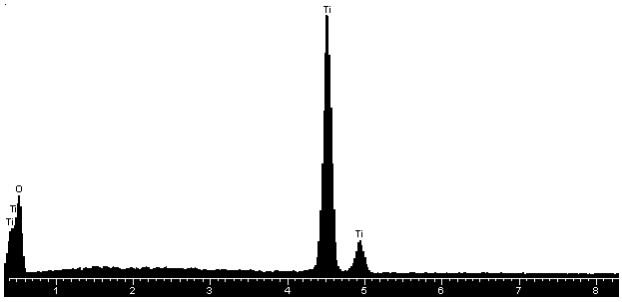

Fig. 3. EDS analysis of the nano-TiO_2 particle

Fig. 5 shows the degradation of alizarin salt (AS) dye. Alizarin salt dye was tested using the anatase phased nano-TiO_2 as catalyst under UV irradiation. The extent of degradation of alizarin salt dye was followed by UV-vis spectroscopy. The spectra of the AS-1 h and AS-2 h show of the absorption low from the alizarin salt which can be assigned at range 240 and 520 nm.

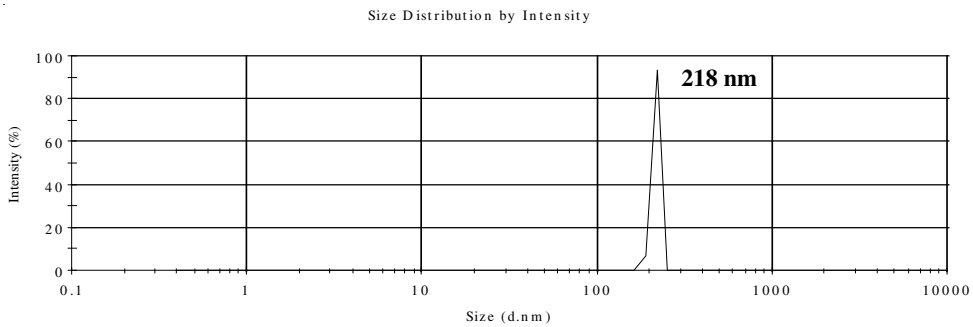

Fig. 4. Particle size distribution in the aqua atmosphere

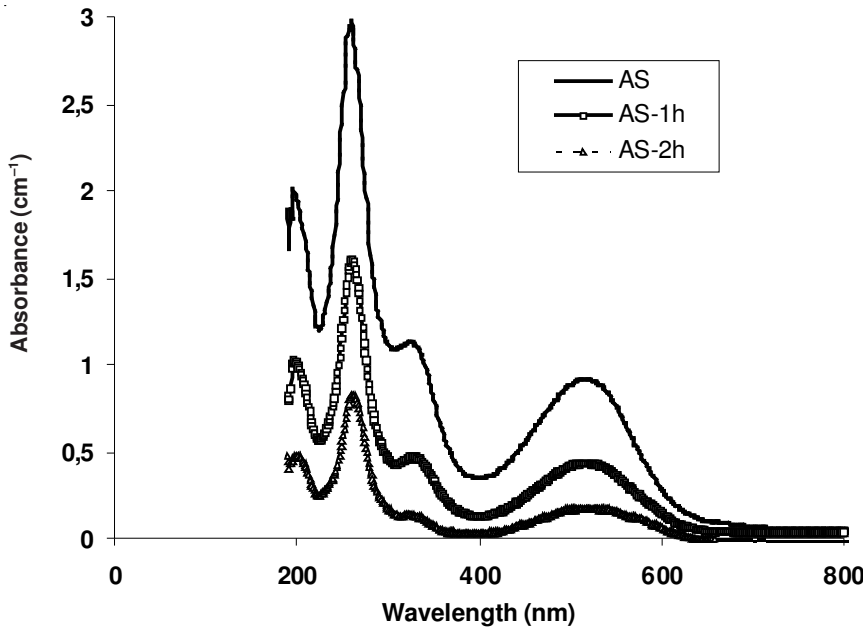

Fig. 5. UV-vis absorption of degradation of alizarin salt (AS)

Conclusion

Pure TiO_2 with an 10 nm crystallite size was synthesized hydrothermally at 200 ºC in 90 min. Anatase was the only crystalline phase in the nano-TiO_2 powder. Transparent TiO_2 stainless steel plates were prepared by dip coating technique. The activity of the synthesized anatase-TiO_2 in catalytic degradation of alizarin under UV-light was examined and found that it is an efficient catalysis to complete degradation of higher concentrations of alizarin salt dye in very short irradiation time. Oxidation conditions were determined for photocatalytic degradation of alizarine salt dye. For initial concentration of 30.0 mgL^{-1} alizarin in 1 wt. % TiO_2 sol, the apparent reaction rate constant was 0.080 min^{-1} and the half period of alizarin degradation was nearly 70.0 min.

REFERENCES

1. N. Venkatachalam, M. Palanichamy and V. Murugesan, *Mater. Chem. Phys*., **104**, 454 (2007).
2. F. Sayilkan, M. Asilturk, S. Erdemoglu, M. Akarsu, H. Sayilkan, M. Erdemoglu and E. Arpac, *Mater. Lett*., **60**, 230 (2006).
3. A. Nasu and Y. Otsubo, *J. Colloid. Interface Sci*., **296**, 558 (2006).
4. G. Wang, *J. Molecul. Catal. A: Chem*., **274**, 185 (2007).
5 J. Wang, T. Ma, G. Zhang, Z. Zhang, X. Zhang, Y. Jiang, G. Zhao and P. Zhang, *Catal. Commun*., **8**, 607 (2007).
6. G. Tian, H. Fu, L. Jing and C. Tian, *J. Hazard. Mater*., **161**, 1122 (2009).
7. C. Sarantopoulos, A.N. Gleizes, F. Maury, *Sur. Coat. Tech*., **201**, 9354 (2007).
8. B. Mounir, M.N. Pons, O. Zahraa, A. Yaacoubi and A. Benhammou, *J. Hazard. Mater*., **148**, 513 (2007).
9. S. Kurinobu, K. Tsurusaki, Y. Natui, M. Kimata and M. Hasegawa, *J. Magnetism Magnetic Mater*., **310**, 1025 (2007).
10. A.C. Pierre, Introduction to Sol-Gel Processing, Kluwer Academic Publishers (1998).
11. C.J. Brinker and G.W. Scherer, The Physics and Chemistry of Sol-gel Processing, Academic Press (1989).
12. J. Wang, W. Sun, Z. Zhang, Z. Xing, R. Xu, R. Li, Y. Li and X. Zhang, *Ultraso. Sonochem*., **15**, 301 (2008).
13. H. Sayilkan, *Appl. Catal. A: General*, **319**, 230 (2007).
14. S. Chiu, Z. Chen, K. Yang, Y. Hsuc and D. Gana, *J. Mater. Proc. Tech*., **192**, 60 (2007).
15. S.F. Villanueva and S.S. Martinez, *Solar Ener. Mater. Solar Cells*, **91**, 1492 (2007).
16. B. Mounir, M.N. Pons, O. Zahraaand, A. Yaacoubi, A. Benhammou, *J. Hazard. Mater*., **148**, 513 (2007).
17. S. Mozia, M. Tomaszewska and A.W. Morawski, *Catal. Today*, **129**, 3 (2007).
18. A. Guevara-Lara, R. Bacaud and M. Vrinat, *Appl. Catal. A: General*, **328**, 99 (2007).
19. W. Suchanek, M.M. Lencka and R.E. Riman, *Acta Medica*, **49**, 129 (2006).
20. S. Somiya and R. Roy, *Bull. Mater. Sci*., **23**, 453 (2000).
21. C. Kaya, J.Y. He, X. Gu and E.G. Butler, *Micro. Mesopo. Mater*., **54**, 37 (2002).
22. F. Sayilkan, S. Erdemoglu, M. Asilturk, M. Akarsu, S. Sener, H. Sayilkan, M. Erdemoglu and E. Arpac, *Mater. Res. Bull*., **41**, 2276 (2006).
23. M. Asilturk, F. Sayilkan, S. Erdemoglu, M. Akarsu, H. Sayilkan, M. Erdemoglu and E. Arpac, *J. Hazar. Mater*., **129**, 164 (2006).
24. S. Kurinobu, K. Tsurusaki, Y. Natui, M. Kimata and M. Hasegawa, *J. Magnet. Magnetic Mater*., **310**, 1025 (2007).

(*Received*: 13 June 2009; *Accepted*: 24 December 2009) AJC-8225